

Sulfonated covalent organic framework packed nafion membrane with high proton conductivity for H₂/O₂ fuel cell applications

Zhichao Shao^{+,a} Xiaojing Xue^{+,b} Kexin Gao,^a Junshuai Chen,^a Lipeng Zhai,^{*a} Tianyang Wen,^b Shenglin Xiong,^c Hongwei Hou^{*b} and Liwei Mi^{*a}

^aCenter for Advanced Materials Research, Zhongyuan University of Technology, Zhengzhou 450007, P. R. China. E-mail: zhailp@zut.edu.cn, mlwzzu@163.com.

^bCollege of Chemistry, Zhengzhou University, Zhengzhou, Henan, 450001, P. R. China. E-mail: houhongw@zzu.edu.cn.

^cSchool of Chemistry and Chemical Engineering, Shandong University, Jinan, 250100, P. R. China.

Supporting Information

Fig. S1 Infrared spectrum of ZUT-COF-SO₃H.

Fig. S2 Solid state ¹³C NMR of ZUT-COF-SO₃H.

Fig. S3 Thermogravimetric analysis of ZUT-COF-SO₃H.

Fig. S4 SEM and mapping images of ZUT-COF-SO₃H.

Fig. S5 XPS spectrum of ZUT-COF-SO₃H.

Fig. S6 The distance between different layers in the AA stacking mode.

Fig. S7 The photos of sample preparation and test equipment.

Fig. S8 Impedance spectra of ZUT-COF-SO₃H at different humidity.

Fig. S9 Activation energy of ZUT-COF-SO₃H at different humidity.

Fig. S10 Arrhenius curve of ZUT-COF-SO₃H at different humidity.

Fig. S11 Temperature-dependent proton conductivity of ZUT-COF-SO₃H.

Fig. S12 SEM and EDS of ZUT-COF-SO₃H@Nafion cross section.

Fig. S13 Infrared spectrum of ZUT-COF-SO₃H@Nafion hybrid membranes.

Fig. S14 Thermogravimetric analysis of 10%ZUT-COF-SO₃H@Nafion hybrid membranes.

Fig. S15 Water contact angle of 10%-ZUT-COF-SO₃H@Nafion.

Fig. S16 Impedance spectra of ZUT-COF-SO₃H@Nafion hybrid membranes at 80%RH.

Fig. S17 Activation energy of ZUT-COF-SO₃H@Nafion hybrid membranes at different humidity.

Fig. S18 Proton conductivity of ZUT-COF-SO₃H@Nafion hybrid membranes.

Fig. S19 Temperature-dependent proton conductivity of hybrid membranes.

Fig. S20 Impedance spectra of 10%ZUT-COF-SO₃H@Nafion hybrid membranes at different humidity.

Fig. S21 Activation energy of 10%ZUT-COF-SO₃H@Nafion hybrid membranes at different humidity.

Fig. S22 Arrhenius curve of 10%ZUT-COF-SO₃H@Nafion hybrid membranes at different humidity.

Fig. S23 Proton conductivity of 10%ZUT-COF-SO₃H@Nafion hybrid membranes.

Table S1 Performance comparisons of proton conductivity with other reported materials.

Table S2 Performance comparisons of power density with other reported materials.

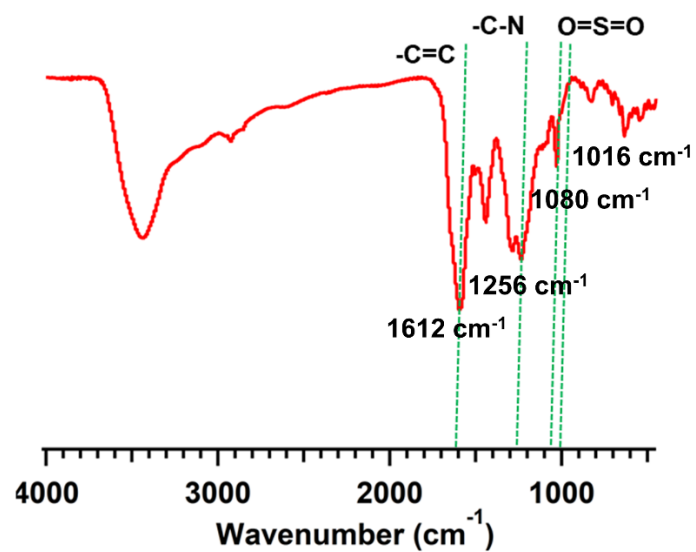


Fig. S1 Infrared spectrum of ZUT-COF-SO₃H.

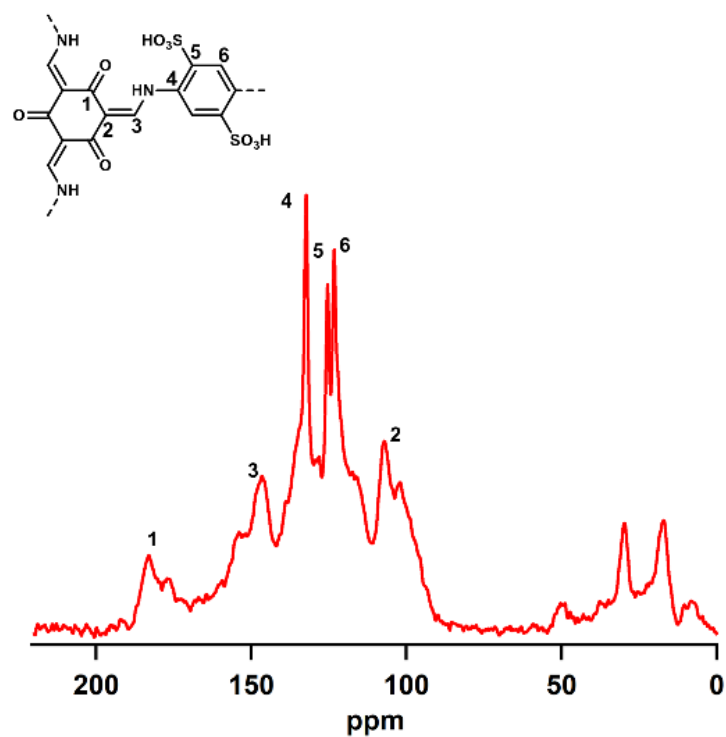


Fig. S2 Solid state ¹³C NMR of ZUT-COF-SO₃H.

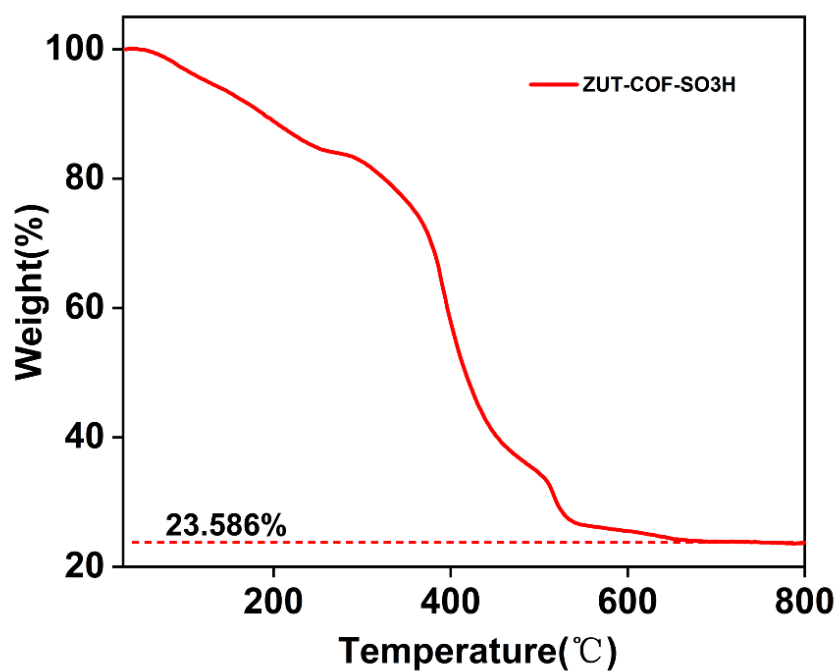


Fig. S3 Thermogravimetric analysis of ZUT-COF-SO₃H.

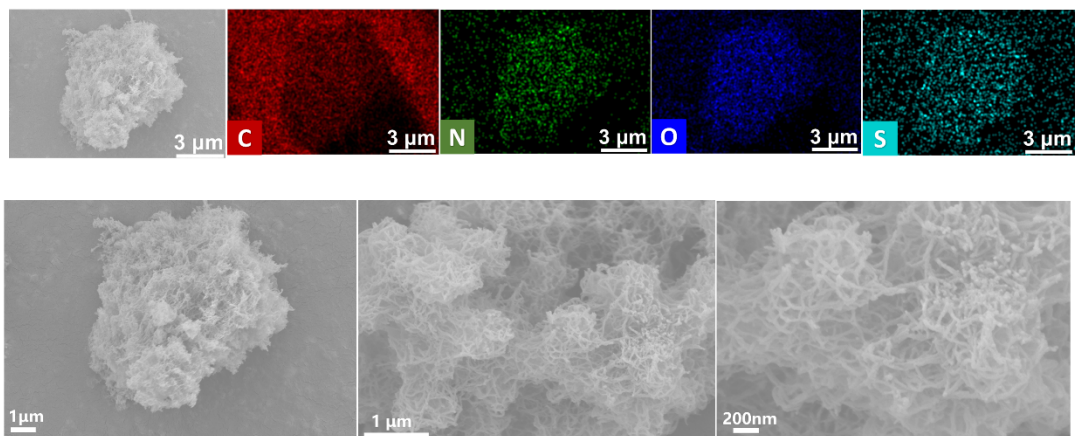


Fig. S4 SEM and mapping images of ZUT-COF-SO₃H.

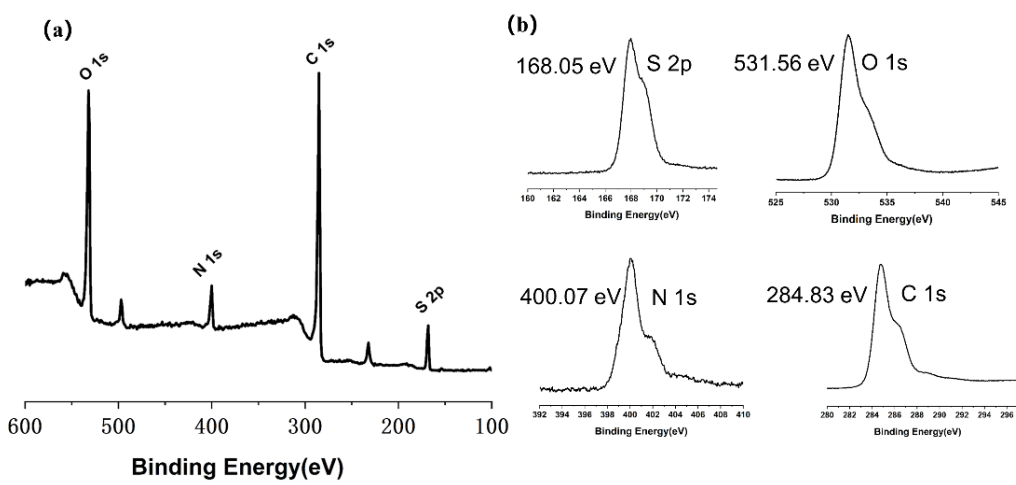


Fig. S5 XPS spectrum of ZUT-COF-SO₃H.

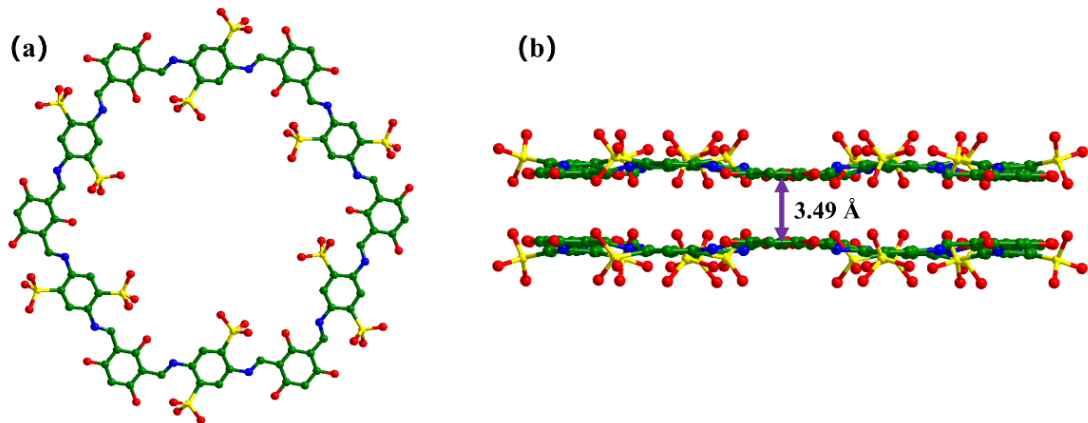


Fig. S6 The distance between different layers in the AA stacking mode.

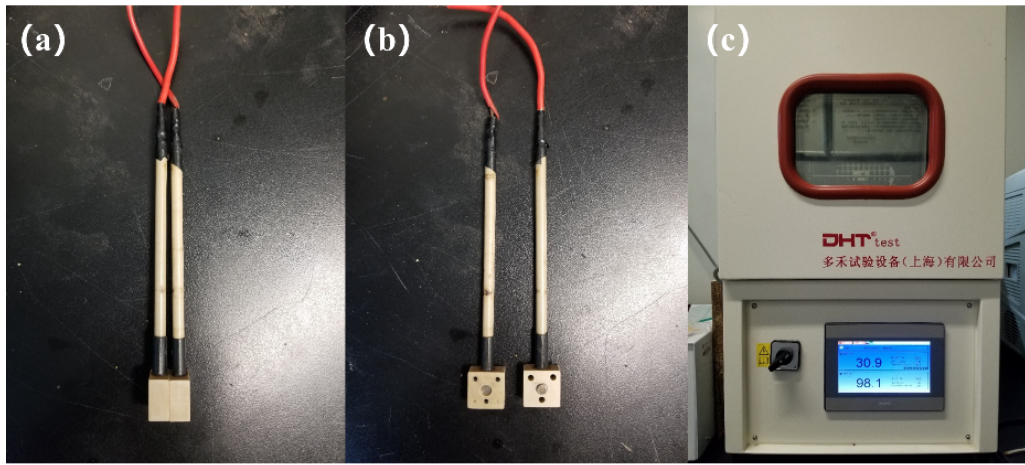


Fig. S7 Sample preparation and test equipment: (a, b) test electrode, (c) constant temperature and humidity oven.

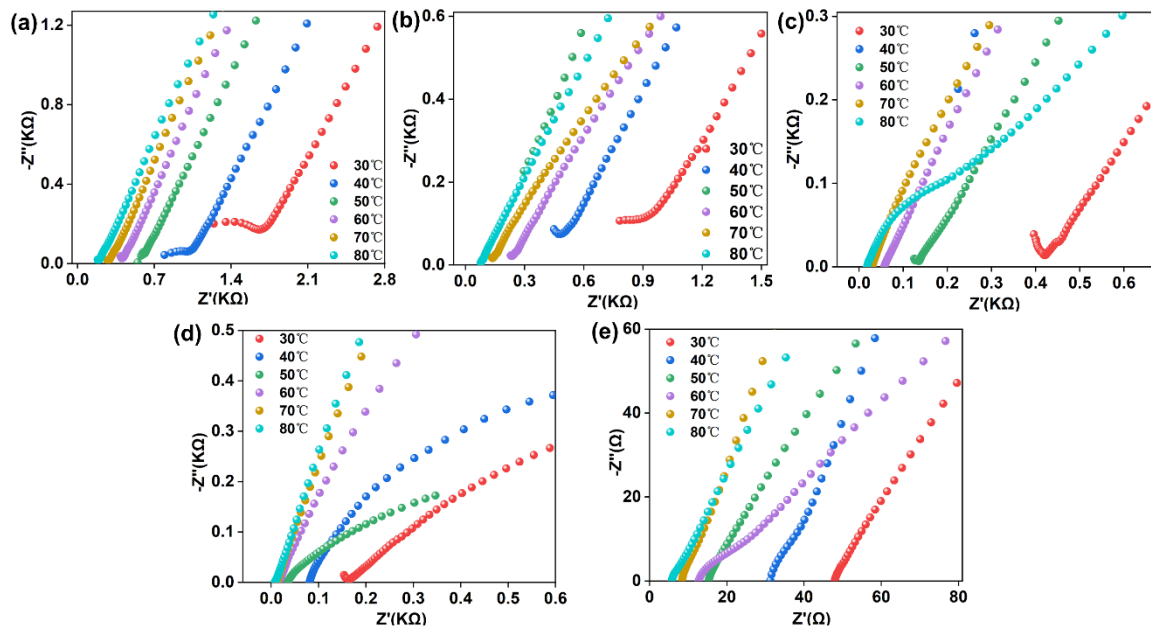


Fig. S8 Impedance spectra of ZUT-COF-SO₃H at different humidity, (a) 60%, (b) 70%, (c) 80%, (d) 90%, (e) 98%.

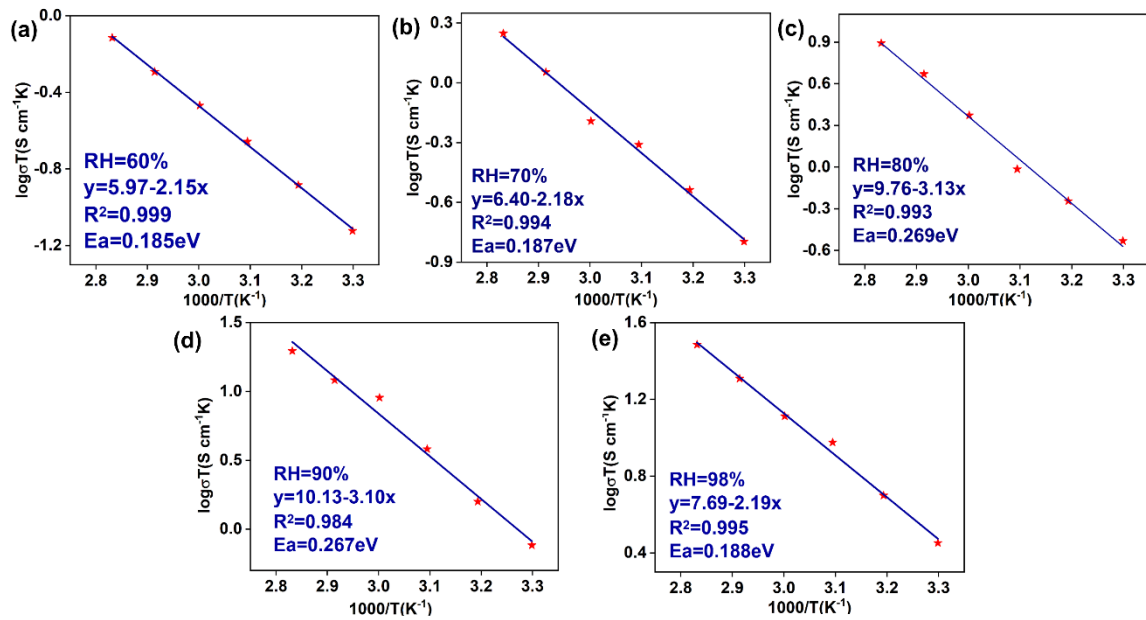


Fig. S9 Activation energy of ZUT-COF-SO₃H at different humidity,(a)60%, (b)70%, (c)80%, (d)90%, (e)98%.

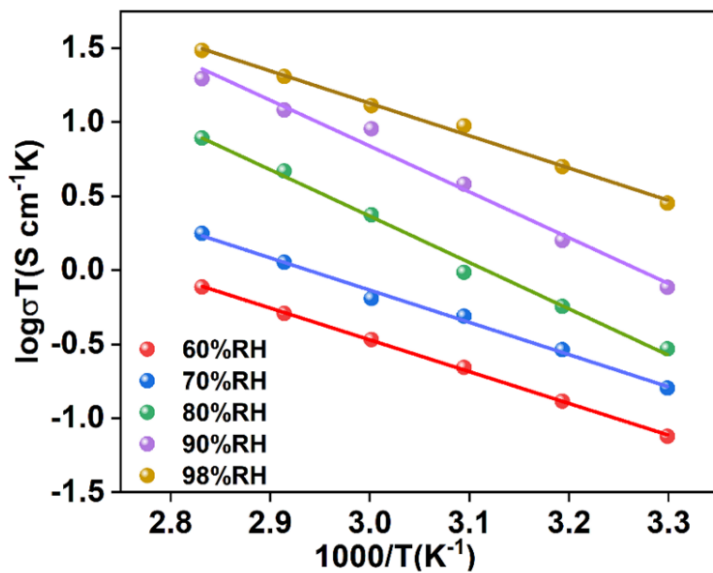


Fig. S10 Arrhenius curve of ZUT-COF-SO₃H at different humidity.

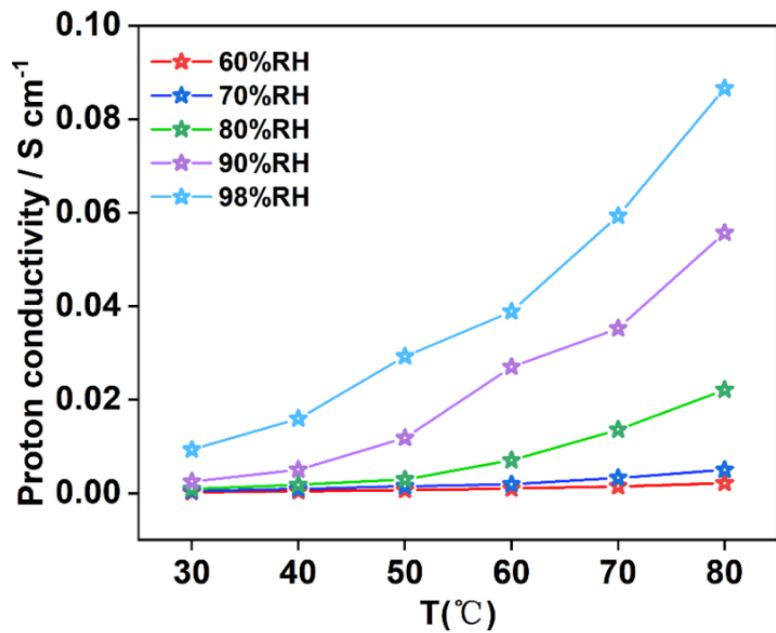


Fig. S11 Temperature-dependent proton conductivity of ZUT-COF-SO₃H.

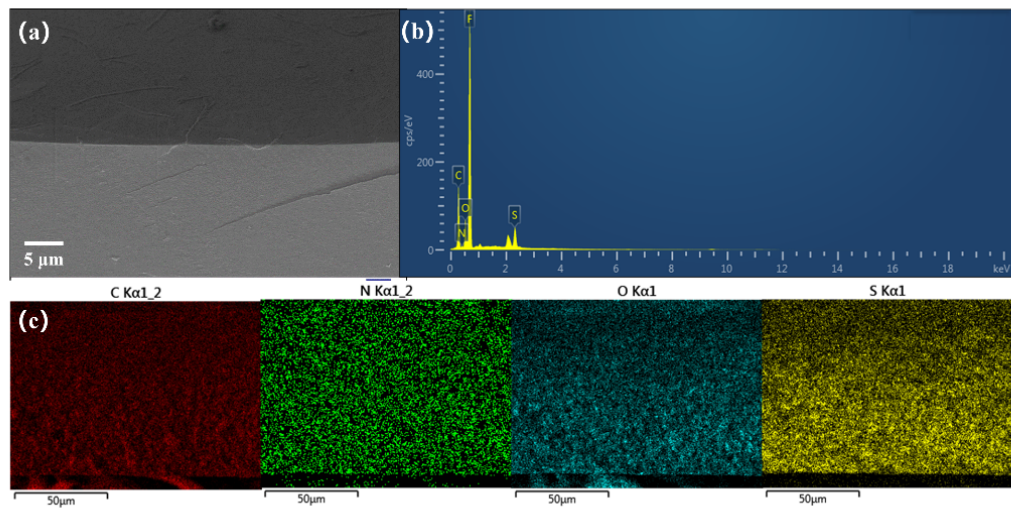


Fig. S12 SEM and EDS of ZUT-COF-SO₃H@Nafion cross section.

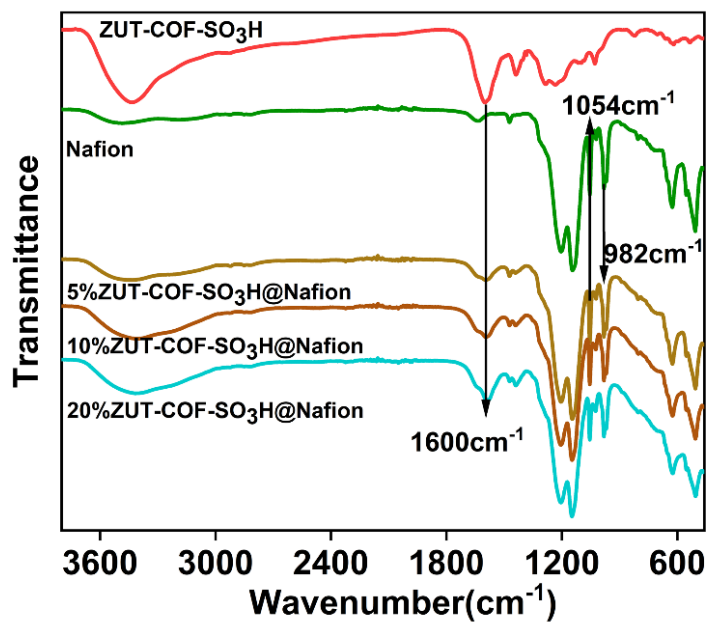


Fig. S13 Infrared spectrum of ZUT-COF-SO₃H@Nafion hybrid membranes.

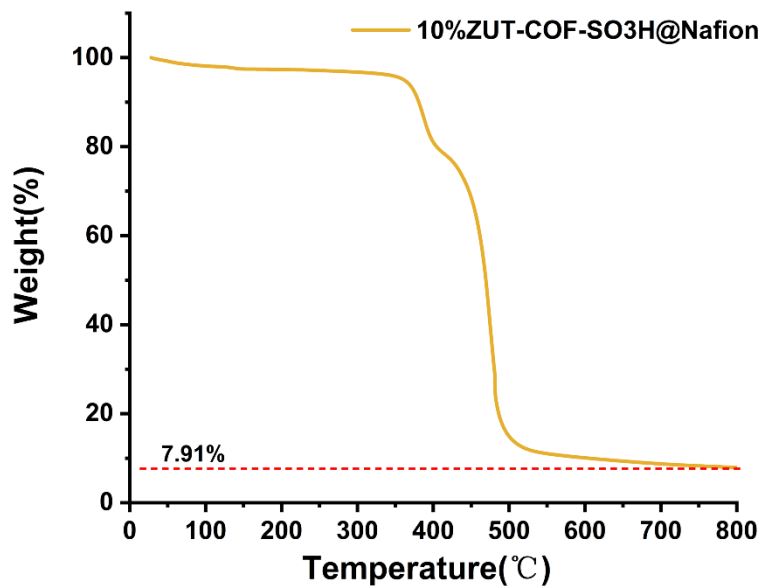


Fig. S14 Thermogravimetric analysis of 10%ZUT-COF-SO₃H@Nafion hybrid membranes

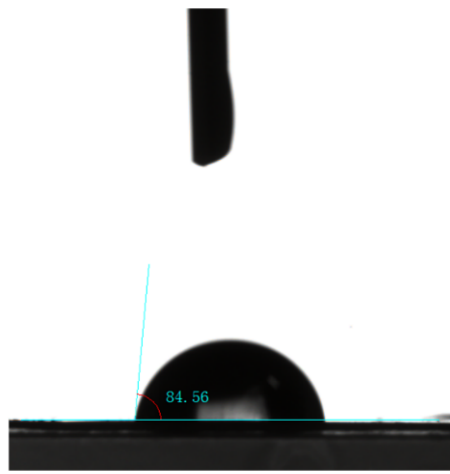


Fig. S15 Water contact angle of 10%-ZUT-COF-SO₃H@Nafion.

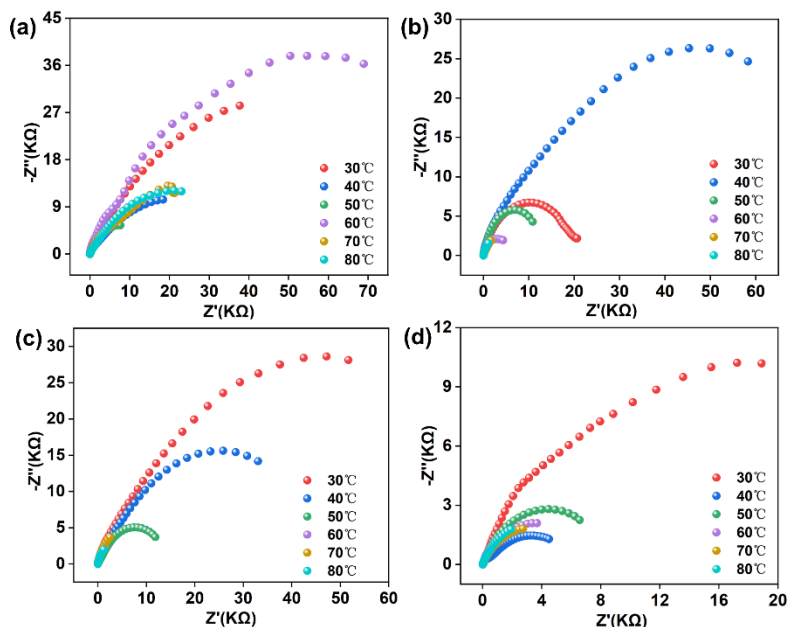


Fig. S16 Impedance spectra of ZUT-COF-SO₃H@Nafion hybrid membranes with different loading at 80%RH, (a)0%, (b) 5%, (b) 10%, (b)20%.

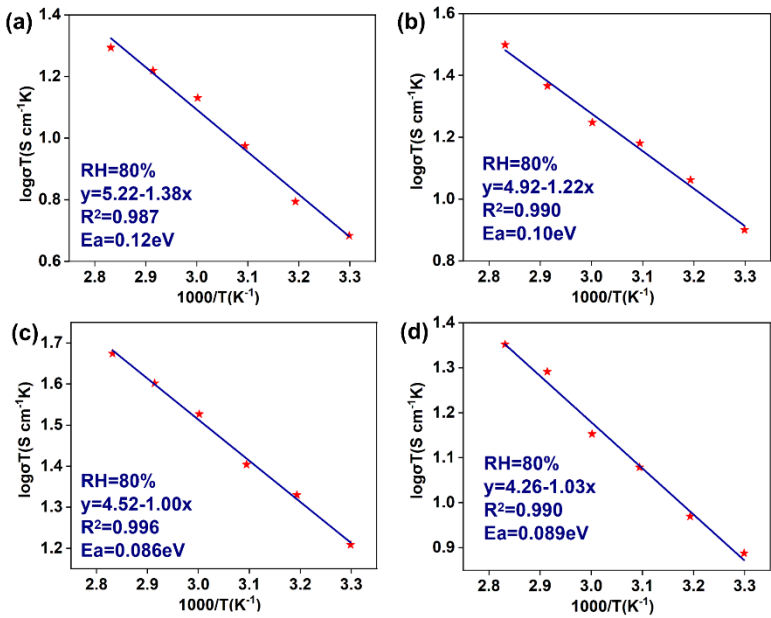


Fig. S17 Activation energy of ZUT-COF-SO₃H@Nafion hybrid membranes with different loading
(a)0%, (b) 5%, (b) 10%, (b)20%.

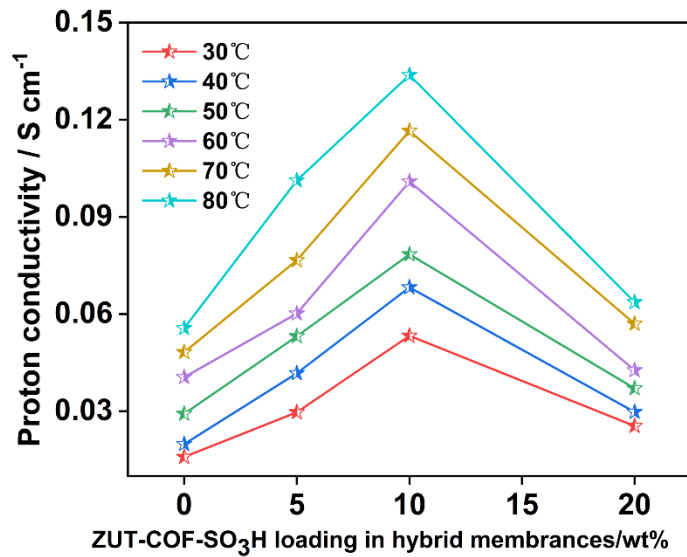


Fig. S18 Proton conductivity of ZUT-COF-SO₃H@Nafion hybrid membranes with different loading.

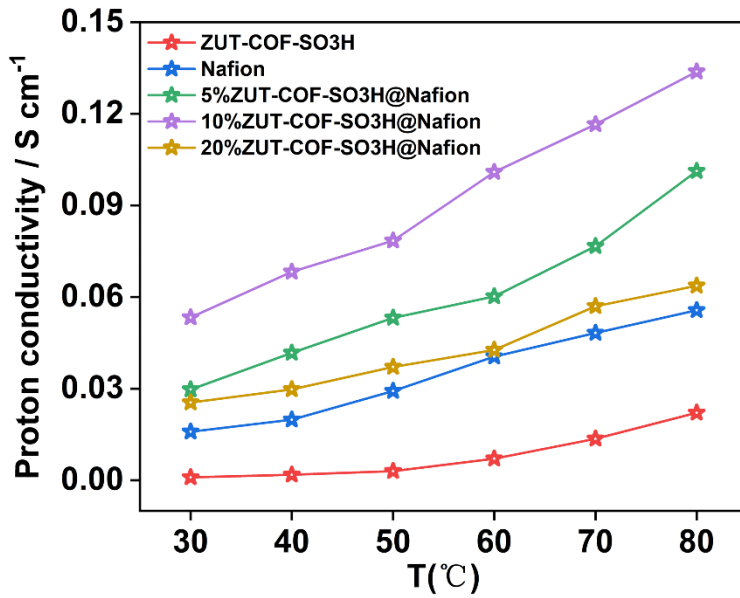


Fig. S19 Temperature-dependent proton conductivity of ZUT-COF-SO₃H@Nafion hybrid membranes with different loading.

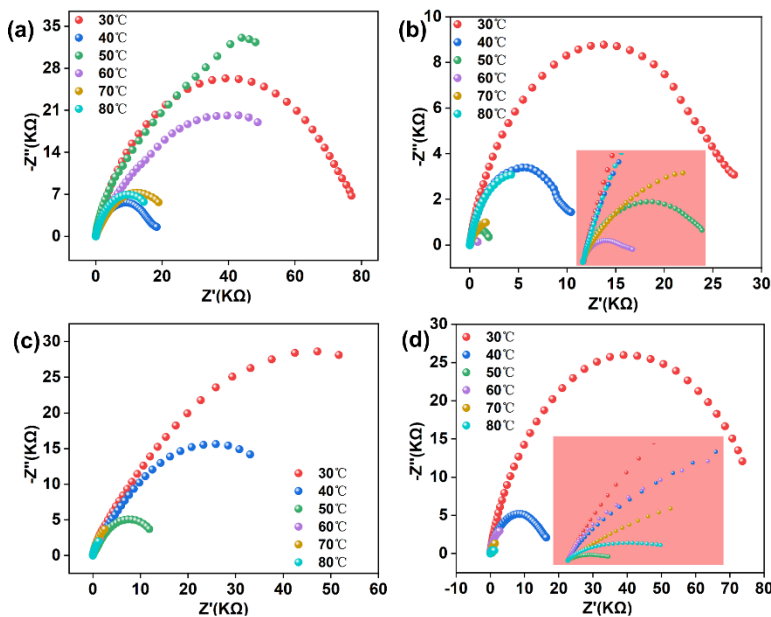


Fig. S20 Impedance spectra of 10%ZUT-COF-SO₃H@Nafion hybrid membranes at different humidity, (a)60%, (b)70%, (c)80%, (d)90%.

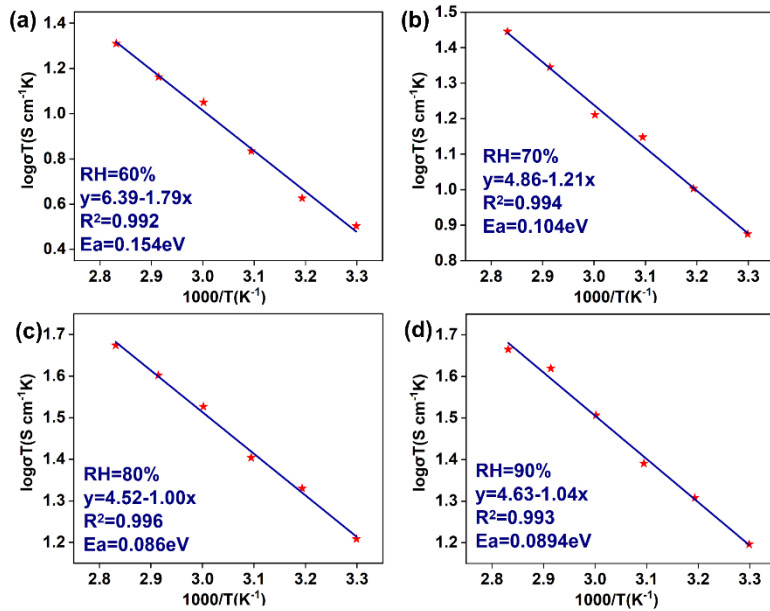


Fig. S21 Activation energy of 10%ZUT-COF-SO₃H@Nafion hybrid membranes at different humidity, (a)60%, (b)70%, (c)80%, (d)90%.

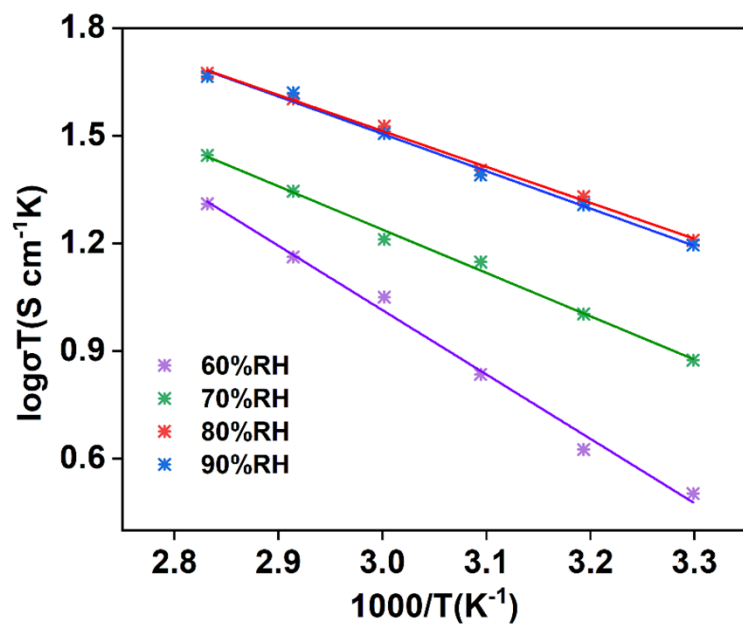


Fig. S22 Arrhenius curve of 10%ZUT-COF-SO₃H@Nafion hybrid membranes at different humidity.

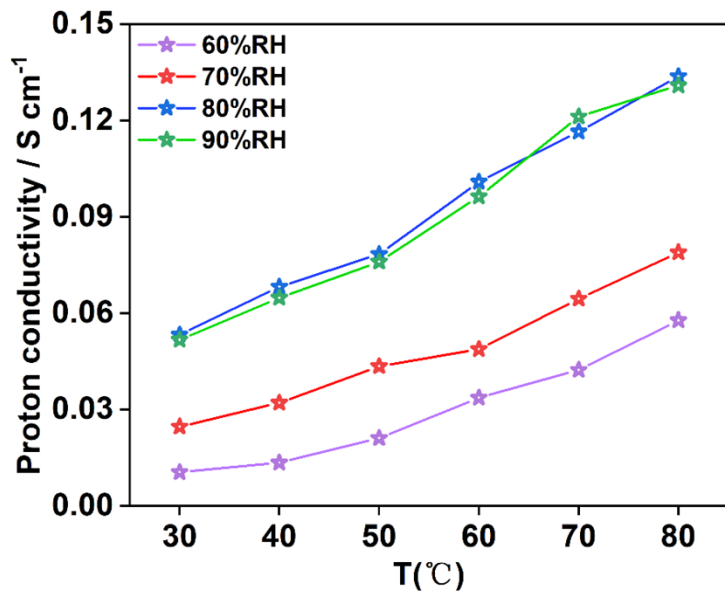


Fig. S23 Proton conductivity of 10%ZUT-COF-SO₃H@Nafion hybrid membranes.

Table S1 Performance comparisons of proton conductivity with other reported material.

Materials	Proton conductivi	Test environment	Reference
MIL-101-SO ₃ H	1.16×10 ⁻²	100%RH, 80 °C	S1
KAUST-7'	2.2×10 ⁻²	95%RH, 90 °C	S2
{[Cu ₃ L ₂ (H ₂ O) ₆]·2H ₂ O} _n	4.08×10 ⁻³	100%RH, 95 °C	S3
B-PCMOF-2	1.3×10 ⁻³	90%RH, 85 °C	S4
Mg(p-BDC)(PyOH)_Cs	1.61×10 ⁻²	90%RH, 90 °C	S5
{[Fe ^{III} ₃ L ₂ (H ₂ O) ₆]•3(OH)} _n /PVP/PVDF-10	1.77×10 ⁻³	98%RH, 80 °C	S6
N_U ₂₀₀ -2	1.65×10 ⁻¹	95%RH, 80 °C	S7
N_U ₂₀₀ -10	7.9×10 ⁻²	95%RH, 80 °C	S7
TpBD-(SO ₃ H) ₂ iCOFs	6.6×10 ⁻¹	100%RH, 90 °C	S8
BIY-COF	1.9×10 ⁻²	95%RH, 95 °C	S9
TFPPY-BT-COF-H ₂ PO ₃	1.12×10 ⁻³	98%RH, 60 °C	S10
TFPPY-PDA-COF-H ₂ PO ₃	1.34×10 ⁻⁴	98%RH, 60 °C	S10
Nafion	~1×10 ⁻¹	98%RH, 80 °C	S11
BIP-COF	3.2×10 ⁻²	95%RH, 95 °C	S12
H ₃ PO ₄ @NKCOF-1	1.13×10 ⁻¹	98%RH, 80 °C	S13
H ₃ PO ₄ @NKCOF-2	4.28×10 ⁻²	98%RH, 80 °C	S13
H ₃ PO ₄ @NKCOF-3	1.12×10 ⁻²	98%RH, 80 °C	S13
H ₃ PO ₄ @NKCOF-4	7.71×10 ⁻²	98%RH, 80 °C	S13
aza-COF-1H	1.23×10 ⁻³	97%RH, 50 °C	S14
aza-COF-2H	4.8×10 ⁻³	97%RH, 50 °C	S14
RT-COF-1Ac	1.07×10 ⁻⁴	100%RH, 40 °C	S15
PTSA@TpAzoCOFM	7.8×10 ⁻²	95%RH, 80 °C	S16
ZUT-COF-SO₃H	8.65×10⁻²	98%RH, 80 °C	This work
10%ZUT-COF-SO₃H@Nafion	1.338×10⁻¹	80%RH, 80 °C	This work

Table S2 Performance comparisons of power density with other reported materials.

Samples	Power Density mW cm ⁻²	Ref.
SPEEK/2#-10	104.5	<i>Adv. Funct. Mater.</i> 2012, 22 , 4539–4546
RN-PQD-5%	407	<i>Adv. Mater.</i> 2018, 30 , 1707516
SPEEK/HPW@mGO-4	120.1	<i>Ind. Eng. Chem. Res.</i> 2021, 60 , 4460–4470
QOPBI-15	260	<i>J. Membr. Sci.</i> 2020, 593 , 117435
OPBI	190	
SPAES/ATP\ P-CNOs-2	752	<i>J. Membr. Sci.</i> 2022, 660 , 120774
PANI-30%-OPBI	250	<i>Journal of Power Sources</i> , 2022, 528, 231218
10%-ILs/NH ₂ -CNTs/OPBI	291	<i>Journal of Power Sources</i> , 2022, 543, 231802
ImPOSS-Nafion	246	<i>RSC Adv.</i> , 2013, 3 , 5438–5446
M-3#/PA	280	<i>Ind. Eng. Chem. Res.</i> 2017, 56 , 10227–10234
10%ZUT-COF-SO₃H@Nafion	304.056	This work

References

- [S1] S. N. Zhao, X. Z. Song, M. Zhu, X. Meng, L. L. Wu, S. Y. Song, C. Wang and H. J. Zhang, *Dalton Trans.*, 2015, **44**, 948–954.
- [S2] X. Wang, Y. L. Wang, M. A. Silver, D. X. Gui, Z. L. Bai, Y. X. Wang, W. Liu, L. H. Chen, J. D. Wu, Z. F. Chai and S. A. Wang, *Chem. Commun.*, 2018, **54**, 4429–4432.
- [S3] D. A. Levenson, J. F. Zhang, P. M. J. Szell, D. L. Bryce, B. S. Gelfand, R. P. S. Huynh, N. D. Fylstra, and G. K. H. Shimizu, *Chem. Mater.*, 2020, **32**, 679–687.
- [S4] H. F. Wang, Q. Wu, X. Y. Ding, Z. C. Shao, W. J. Xu, Y. J. Zhao, Q. Xie, X. R. Meng, and H. W. Hou, *Inorg. Chem.*, 2020, **59**, 8361–8368.
- [S5] S. Kim, B. Joarder, J. A. Hurd, J. Zhang, K. W. Dawson, B. S. Gelfand, N. E. Wong, and G. K. H. Shimizu, *J. Am. Chem. Soc.*, 2018, **140**, 1077–108.
- [S6] T. Y. Wen, Z. C. Shao, H. F. Wang, Y. J. Zhao, Y. Cui, and H. W. Hou, *Inorg. Chem.*, 2021, **60**, 18889–18898.
- [S7] A. Donnadio, R. Narducci, M. Casciola, F. Marmottini, R. D’Amato, M. Jazestani, H. Chiniforoshan, and F. Costantino, *ACS Appl. Mater. Interfaces*, 2017, **9**, 42239–42246.
- [S8] X. Y. Wang, B. B. Shi, H. Yang, J. Y. Guan, X. Liang, C. Y. Fan, X. D. You, Y. A. Wang, Z. Zhang, H. Wu, T. Cheng, R. N. Zhang and Z. Y. Jiang, *Nat Commun.*, 2022, **13**, 1020.
- [S9] S. Z. Yang, C. Q. Yang, C. C. Dun, H. Y. Mao, R. S. H. Khoo, L. M. Klivansky, J. A. Reimer, J. J. Urban, J. Zhang, and Y. Liu, *J. Am. Chem. Soc.*, 2022, **144**, 9827–9835.
- [S10] Z. W. Lu, C. Y. Yang, L. He, J. Hong, C. H. Huang, T. Wu, X. Wang, Z. F. Wu, X. H. Liu, Z. X. Miao, B. R. Zeng, Y. T. Xu, C. H. Yuan, and L. Z. Dai, *J. Am. Chem. Soc.*, 2022, **144**, 9624–9633.
- [S11] X. M. Wu, X. W. Wang, G. H. He, J. Benziger, *J. Polym. Sci. B Polym. Phys.*, 2011, **49**, 1437–1445.
- [S12] K. C. Ranjeesh, R. Illathvalappil, S. D. Veer, J. Peter, V. C. Wakchaure, Goudappagouda, K. V. Raj, S. Kurungot, and S. S. Babu, *J. Am. Chem. Soc.*, 2019, **141**, 14950–14954.
- [S13] Y. Yang, X. Y. He, P. H. Zhang, Y. H. Andalousi, H. Zhang, Z. Y. Jiang, Y. Chen, S. Q. Ma, P. Cheng, and Z. J. Zhang, *Angew. Chem. Int. Ed.*, 2020, **59**, 3678–3684.
- [S14] Z. Meng, A. Aykanat, and K. A. Mirica, *Chem. Mater.*, 2019, **31**, 819–825.
- [S15] C. Montoro, D. R. S. Miguel, E. Polo, R. E. Cid, M. L. R. Gonzalez, J. A. R. Navarro, P. Ocon, and F. Zamora, *J. Am. Chem. Soc.*, 2017, **139**, 10079–10086.
- [S16] H. S. Sasmal, H. B. Aiyappa, S. N. Bhange, S. Karak, A. Halder, S. Kurungot, and R. Banerjee, *Angew. Chem. Int. Ed.*, 2018, **57**, 10894–10898.